Variation of Moho depth in the central part of the Alborz Mountains, northern Iran

A. Radjaee, D. Rham, M. Mokhtari, M. Tatar, K. Priestley, D. Hatzfeld

Geophys. J. Int. (2010) **181,** 173–184 doi: 10.1111/j.1365-246X.2010.04518.x

Variation of Moho depth in the central part of the Alborz Mountains, northern Iran

A. Radjaee,[1] D. Rham,[2] M. Mokhtari,[1] M. Tatar,[1] K. Priestley[2] and D. Hatzfeld[3]

[1] *International Institute of Earthquake Engineering and Seismology, Tehran, Iran*
[2] *Department of Earth Sciences, University of Cambridge, Cambridge, UK. E-mail: keith@madingley.org*
[3] *Laboratoire de Geophysique Interne et Tectonophysique de Grenoble, University Joseph Fourier, Grenoble, France*

Accepted 2010 January 11. Received 2010 January 9; in original form 2009 September 9

SUMMARY

The Alborz Mountains of northern Iran form a belt of active crustal deformation along the southern side of the Caspian Sea within the broad Arabian–Eurasia continental collision zone. Although the range has an average elevation of about 3000 m with the volcanic peak Damavand reaching an elevations of 5671 m, early gravity studies found that the crust beneath the range is no thicker than that beneath the surrounding region suggesting the range is not supported by a crustal root. We determine a model for the crust of the central Alborz Mountains using teleseismic receiver functions from data recorded on a network of broad-band seismographs temporarily deployed across the central part of the range. The receiver functions from these recordings have been inverted simultaneously with fundamental-mode Rayleigh wave group velocity measurements in the 10–100 s period range. Our analysis shows a thickening of the crust from ∼48 km beneath the northern part of the Central Iranian Plateau to 55–58 km below the central part of the Alborz Mountains, then a thinning of the crust to ∼46 km north of the Alborz Mountains beneath the coastal region of the South Caspian Sea. Our seismological results show that the central Alborz Mountains have a moderate crustal root but of insufficient thickness to compensate the elevation of the range. The analysis of free-air gravity shows that the elevation of the Alborz Mountains is largely supported by the elastic strength of the Iranian Plate, the South Caspian Plate, or both.

Key words: Continental margins: convergent; Intra-plate processes; Crustal structure.

1 INTRODUCTION

The Alborz Mountains form a seismically active fold-and-thrust belt along the southern Caspian Sea coast extending from the southern end of the Talesh Mountains in the west to their junction with the Kopeh Dagh Mountains in the east (Fig. 1). About a quarter of the overall Arabian-Eurasian convergence in this part of the collision zone ($\sim 5 \pm 2$ mm yr^{-1}) is accommodated across the Alborz Mountains, the remainder occurring in the Zagros Mountains of SW Iran and across the South Caspian Basin (Vernant *et al.* 2004). Most of the focal mechanisms for earthquakes (Fig. 1) in the Alborz show either reverse faulting or left-lateral strike-slip on faults parallel to the regional strike of the range (Priestley *et al.* 1994; Jackson *et al.* 2002). All well-constrained earthquake centroid focal depths in the belt occur at depths shallower than ∼30 km. The Alborz are narrow (120–150 km wide), steep and bounded by major thrust faults on the north (e.g. Khazar Fault) and south (e.g. North Tehran and North Qazvin Faults) sides of the range (Berberian & Yeats 1999) (Fig. 1). The north-bounding reverse faults dip southwards, suggesting the underthrusting of the south Caspian basin (see Tatar *et al.* 2007) and the south-bounding reverse faults dip northwards; both help accommodate shortening between central Iran and stable Eurasia. Strike slip faults occur at higher elevations in the range. Dating of thermal histories of granites in the central Alborz suggests a rapid uplift of the range between about 6 and 4 Ma (Axen *et al.* 2001), nearly synchronous with subsidence in the South Caspian (Allen *et al.* 2004) while others suggest the range is somewhat older (Guest *et al.* 2006; Ballato *et al.* 2008).

Few studies have focused on the crustal structure of Iran, and those that have are primarily concerned with the large-scale structure of the Iranian Plateau and not the detailed structure of the Alborz region. Knowledge of the Moho depth beneath the Alborz Mountains is important for understanding the complex tectonics of northern Iran and for evaluating seismic hazard in the region. The Alborz are a young mountain range (Axen *et al.* 2001; Guest *et al.* 2006; Ballato *et al.* 2008), and earlier gravity analysis (Dehghani & Makris 1984) suggested that the range does not have a crustal root making it unclear what supports the topography.

The seismic hazard in the region is substantial and there is a long history of devastating earthquakes. Towns on the site of the modern capital city of Tehran located on the southern slopes of the Alborz Mountains have been severely damaged or destroyed by

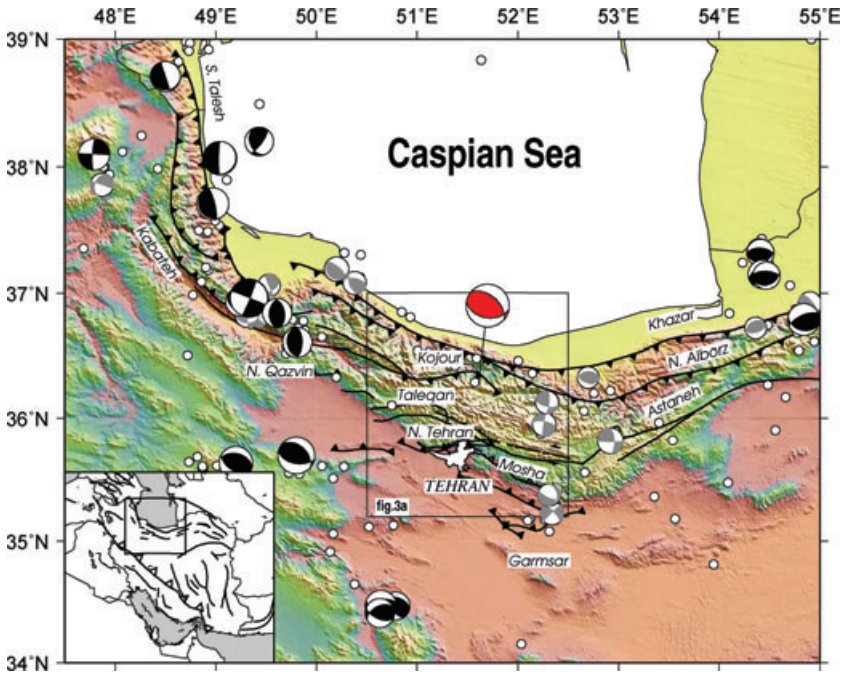

Figure 1. Topography, earthquake locations and focal mechanisms across the Alborz Mountains. Black focal spheres are for earthquakes where the mechanisms are constrained by body waveform modelling (Priestley *et al.* 1994; Jackson *et al.* 2002); grey focal spheres are Harvard CMT solutions for events with $M_w \geq 5.3$ and with ≥70 per cent double-couple component. The red focal spheres is the 2004 Baladeh earthquake whose focal mechanism was also determined by waveform modelling (Tatar *et al.* 2007). Size of the focal spheres are proportional to magnitude. White circles are seismicity from Engdahl *et al.* (2006). The known major faults in the region are indicated. The inset map at lower left shows the location of the central Alborz Mountains with respect to the more broad-scale features of the Arabian–Eurasian collision zone. The box denotes the location of the temporary seismic network in the central Alborz Mountains.

major earthquakes in the fourth century BC, and in 855, 958, 1177 and 1830 AD (Ambraseys & Melville 1982; Berberian & Yeats 1999). A devastating M_w 7.3 earthquake in the Alborz occurred in 1990 near Rudbar (∼40000 deaths) (Berberian *et al.* 1992), and another destructive M_w 6.2 event occurred in 2004 close to Tehran (Tatar *et al.* 2007). Many parts of the northern and southern slopes of the Alborz Mountains are densely populated. Tehran has the largest population (∼12 million inhabitants) but other major cities include Karaj (∼1 million), Qazvin (∼320 000) and Semnan (∼120 000). A number of the major faults in the central Alborz Mountains are known to be active (Ritz *et al.* 2006) but a better evaluation of the seismic hazard of this region requires accurate earthquake locations which depend on better knowledge of the crustal structure. In this paper we present detailed observations of the variation in crustal velocity and Moho depth beneath the central Alborz Mountains derived from substantial seismic data acquired within the range.

2 DATA AND ANALYSIS

A temporary seismic network of 26 broad-band seismographs (Table 1) was installed between May and November 2003 in a region approximately 100 km E–W by 130 km N–S that extends from the Central Iran Plateau in the south, across the central Alborz Mountains to the shoreline of the Caspian Sea in the north (Fig. 1). Fieldwork was carried out by the International Institute of Earthquake Engineering and Seismology, Bullard Laboratories of University of Cambridge and the Laboratoire de Geophysique Interne et Tectonophysique of the Universite Joseph Fourier. The network consisted of 10 CMG-3TD and 16 CMG-6TD three-component Guralp system seismographs. The data were continuously sampled at 100 samples per second and stamped with GPS time. During the operation of the network we recorded 53 teleseismic earthquakes with magnitude 5.7 or greater, and seismograms of these events with suitably high signal-to-noise ratio constitute the data set for our receiver function analysis. Most of the events were located to the east of the network. Due to instrument malfunction, data were only acquired from 22 of the 26 sites.

Receiver functions are radial waveforms created by deconvolving the vertical component of the seismogram from the radial component to isolate the receiver site effect from the other information contained in the teleseismic *P*-wave coda. Receiver functions allow the determination of the delay time between the direct *P*-waves (*Pp*) and the converted *S*-waves (*Ps*) from a velocity discontinuity beneath the station. The crust–mantle boundary, the Moho, is the most common major velocity discontinuity in the lithosphere. In this study, we are concerned with the depth to the Moho and the large-scale features of the crust. Radial receiver functions were computed using the iterative deconvolution method of Ligorria & Ammon (1999). This technique uses a least-squares minimization of the difference between the observed horizontal seismogram and a predicted signal generated by the convolution of an iteratively updated spike train with the vertical seismogram. The resulting radial component time series corresponds closely to the impulse response of the Earth structure beneath the seismograph site and is called the receiver function (Langston 1979).

We invert the radial receiver functions for crustal structure. To improve the signal-to-noise ratio, the receiver functions were stacked. The *Ps–Pp* delay time of the receiver function (Table 1) depends on the depth to the Moho and the average velocity of the crust; thus, there is a trade-off, and neither the Moho depth nor the average velocity of the crust can be uniquely determined through receiver-function analysis alone. To minimize the trade-off between Moho depth and average crustal velocity, we simultaneously invert the

Table 1. Summary of Alborz Receiver Function results.

Sta.	Sensor type	Lat. (°N)	Long. (°E)	Elev. (m)	Ps-Pp (s)	Number RF	Number stacks	Distance (degrees)	Average Moho depth (km)[a]	Average V_s (km s^{-1})
J2	CMG-3TD	36.122	51.367	2425	6.98 ± 0.47	23	4	30–81	56	3.619
J3	CMG-3TD	36.638	51.392	219	4.42 ± 0.18	12	2	30–80	46	3.613
K1	CMG-3TD	35.405	51.312	1106	6.39 ± 0.22	30	5	30–99	48	3.569
HSB[b]		35.428	51.357		6.0				51	
K2	CMG-3TD	35.963	51.542	2203	6.91 ± 0.42	34	4	30–99	57	3.632
K3	CMG-3TD	36.385	51.780	1545	7.35 ± 0.31	24	5	30–98	56	3.512
L1	CMG-3TD	35.630	51.972	1680	6.91 ± 0.26	27	4	30–81	54	3.592
DMV[b]		35.583	52.028		7.8				67.5	
L2	CMG-3TD	36.103	52.170	1658	7.03 ± 0.39	35	5	29–98	58	3.638
N1	CMG-6TD	36.445	51.910	669	6.08 ± 0.26	21	3	29–80	49	3.569
N3	CMG-6TD	36.408	51.565	1361	6.77 ± 0.47	8	2	60–80	56	3.639
N4	CMG-6TD	36.378	51.253	1242	6.05 ± 0.35	7	4	63–97	52	3.593
N6	CMG-6TD	36.232	51.562	2484	6.23 ± 0.65	16	3	30–79	54	3.620
N7	CMG-6TD	36.210	51.828	2026	5.84 ± 0.35	19	4	29–80	52	3.556
N8	CMG-6TD	36.002	51.308	2007	5.52 ± 0.27	12	2	30–80	50	3.559
N9	CMG-6TD	35.965	51.115	1826	6.21 ± 0.38	21	6	30–96	54	3.579
N10	CMG-6TD	35.590	50.630	1262	6.36 ± 0.25	13	2	31–77	49	3.512
MHD[b]		35.686	50.665		6.4				54.5	
T1	CMG-6TD	36.325	52.125	996	6.65 ± 0.38	22	4	29–80	54	3.640
T3	CMG-6TD	36.327	52.357	372	5.00 ± 0.49	18	4	29–79	58	3.448
T4	CMG-6TD	36.240	52.347	1013	6.01 ± 0.52	8	4	29–77	54	3.619
T5	CMG-6TD	36.193	52.017	1907	6.62 ± 0.57	9	3	39–87	57	3.624
T6	CMG-6TD	35.977	52.297	1761	6.70 ± 0.60	17	4	29–80	56	3.622
T7	CMG-6TD	35.883	52.165	2118	6.49 ± 0.46	13	3	41–77	53	3.593
T9	CMG-6TD	35.448	52.170	1447	6.68 ± 0.33	11	3	30–81	52	3.553

[a]Moho depths referred to the surface.
[b]From table 1 of Sodoudi *et al.* (2009).

P-wave receiver functions with fundamental-mode Rayleigh wave group velocity in the period range 10–100 s for the Alborz region (Rham 2009). The simultaneous inversion of both data sets provides strong constraints on crustal structure since receiver functions are sensitive to discontinuities in the structure but less so to the absolute velocities, whereas the dispersion data are sensitive to the absolute velocities but less so to first-order discontinuities.

In the inversion for the crustal model we start with a finely parametrized initial velocity model with a constant shear wave speed of 4.68 km s^{-1} from the surface to 310 km depth and with the global Earth velocity model AK135 (Kennett *et al.* 1995) at deeper depths. We are only concerned here with the crustal velocity structure; the reason for extending the starting model to such large depths was to not introduce artefacts in the inversion of the surface waves by truncating the model. The lack of a Moho discontinuity in the starting inversion model assures us that the location of the Moho in the resulting inversion model is not biased by an initial choice of a Moho in the inversion starting model, and that the Moho location in the inversion model was dictated by the receiver function and surface wave dispersion data alone. We first simultaneously invert the receiver function and dispersion data using the finely parametrized starting model. The initial inversion models were examined for weak boundaries that straddle discontinuities of similar seismic wave speeds and these layers were then combined to create a more coarsely parametrized model which serves as a new starting model for the next inversion iteration. This process was repeated until we obtained the simplest model in terms of number of layers that matched the major features of the receiver function while simultaneously satisfying the surface wave data. We then tested the model using forward modelling to determine how much the significant features of the model could vary while still giving a satisfactory fit to the receiver function and surface wave dispersion data. We found from these tests that the average uncertainty in the Moho depth was ±2.5 km. Receiver-function and surface wave dispersion inversion results for data from station K3 are shown in Fig. 2; results for the remaining 21 sites are shown in Figs A1–A4.

3 MOHO DEPTH VARIATION BENEATH THE ALBORZ MOUNTAINS

Table 1 and Fig. 3 summarizes the inversion results of the receiver function/surface wave analysis. Fig. 3(a) shows the average Moho depths determined for each site. We interpret the Moho as the depth at which the shear wave velocity reaches sustained values typical of the sub-Moho mantle, and this depth is denoted by heavy arrow in the wave speed versus depth plots in the lower part of Fig. 3(b). Fig. 3(a) shows only marginal thickening of the crust across the Alborz Mountains with a deepening of the Moho from slightly less than 50 km beneath the Central Iranian Plateau south of Tehran to about 55–58 km below the highest part of the range. Along the South Caspian coast the crustal thickness is 50 km or less. Most of the individual crustal models from the receiver-function/surface wave dispersion inversion suggest a mid-crustal interface (Fig. 3b). The evidence for this feature is not strong and it more likely results from a positive velocity gradient in the crust and our simplification of the crustal models. However, the data do not warrant more complex crustal models and our philosophy has been to determine the simplest crustal model in terms of the number of layers required to explain the seismic observations.

We form a crustal cross-section across the Alborz Mountains by projecting our results onto a NS profile along longitude 51.75°E extending from station K1 on the northern part of the Central Iran Plateau to station J3 situated close to southern coast of the Caspian

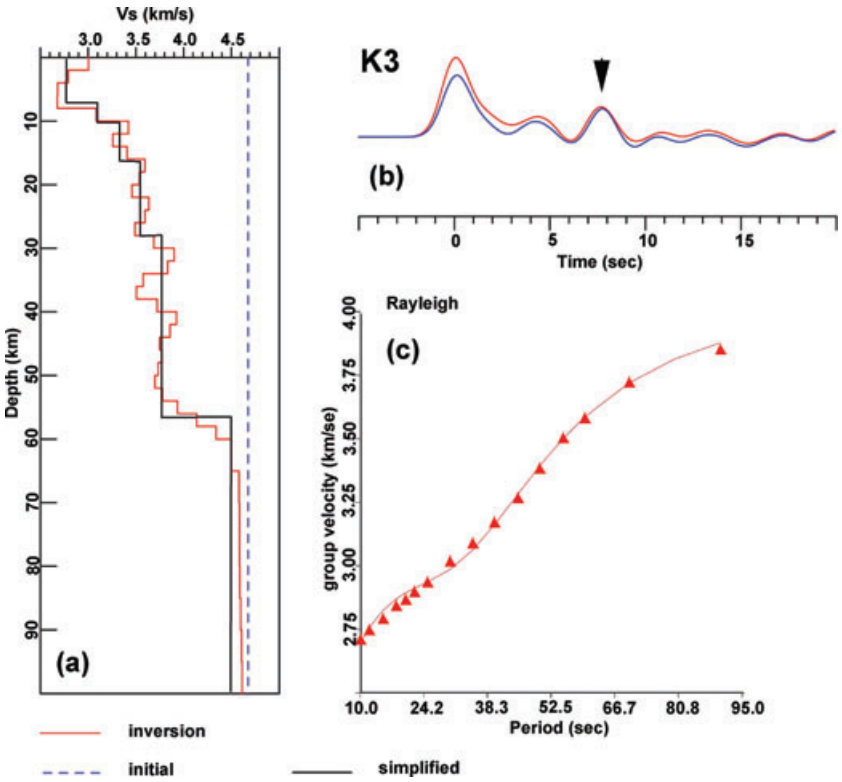

Figure 2. (a) Receiver function/surface wave inversion results for the data from station K3. The dashed blue line denotes the starting model for the iterative inversion, the solid red line denotes the initial, finely parametrized inversion results (2-km-thick layers) and the solid black line denotes the final crustal model consisting of the minimum number of crustal layers required to simultaneously fit the receiver function and surface wave data. (b) The observed stacked radial receiver function for station K3 (blue line) and synthetic (red line) radial receiver function computed for the crustal model shown by the black line in (a). (c) The observed (solid red triangles) group velocity and synthetic (red line) group velocity computed for the crustal model shown by the black line in (a).

Sea (Fig. 3a). The Moho depth along this profile varies from 48 ± 2.5 km at the southern end of the profile on the margin of the Central Iranian Plateau and the Alborz, to 55–58 ± 2.5 km below the central part of the range, to 46 ± 2.5 km near the South Caspian coast. The topography of the mid-crustal interface for the most part mimics the topography of the Moho, the main exception being in the region beneath the highest part of the range in the vicinity of station K2 (Fig. 3b).

4 DISCUSSION

We have determined the crustal velocity structure beneath the central Alborz Mountains of northern Iran by simultaneously inverting data from receiver functions and fundamental mode Rayleigh wave group velocity. These analysis shows a ∼7 km thickening of the crust beneath the central part of the range when compared to the crustal thickness beneath the Central Iran Plateau to the south and beneath the South Caspian Sea coast to the north. From gravity analysis, Dehghani & Makris (1984) found that the crust across north-central Iran was 35–40 km thick and there was little or no crustal root beneath the Alborz Mountains but seismology shows this Moho depth is too shallow. Because their Moho depths were only constrained by gravity, the absolute Moho depths are non-unique. However, except for a rapid thinning of the crust along the South Caspian coast, Dehghani & Makris (1984) do not show a significant variation in crustal thickness across north-central Iran, including beneath the Alborz. Our results show that the crustal thickness beneath the northern part of the Central Iranian Plateau and the Alborz Mountains is 48–58 km, significantly thicker than suggested by their gravity studies. Relative to the northern part of the Central Iranian Plateau, there is a moderate crustal root beneath the Alborz Mountains.

From surface wave analysis Asudeh (1982) suggested that the crust beneath the eastern part of the Alborz Range was ∼45 km but Asudeh's measurements were for a part of the range where the mean elevation is somewhat less than in the central Alborz where our measurements are made. In addition, the paths over which he measured the phase velocity dispersion include a large region of NE Iran and his surface wave observations may not be representative of the central Alborz. On the other hand, Javan & Roberts (2003) found the crust to be ∼46 km beneath the northern part of the Central Iranian Plateau in the region (∼34.5°N, ∼50.75°E) to the south of our central Alborz seismic network, a crustal thickness more compatible with the crustal thickness we find below the southern part of our seismic network. Farther south in central Iran Paul *et al.* (2006) find that the crust of the Central Iranian Plateau is 40–45 km thick.

By far the most comprehensive study of crustal structure in this part of Iran is the receiver function work of Sodoudi *et al.* (2009). They estimated the crustal thickness in the vicinity of Tehran from receiver functions computed from data recorded on 11 short-period seismographs of the Tehran Telemetry Seismic Network. They did not invert the receiver functions for the crustal velocity structure but estimated the Moho depth by converting the *Ps* delay time to depth using the IASPIE91 earth model. Most of the data analysed by Sodoudi *et al.* (2009) come from sites located on the southern flank or south of the Alborz. For the part of the range they sample,

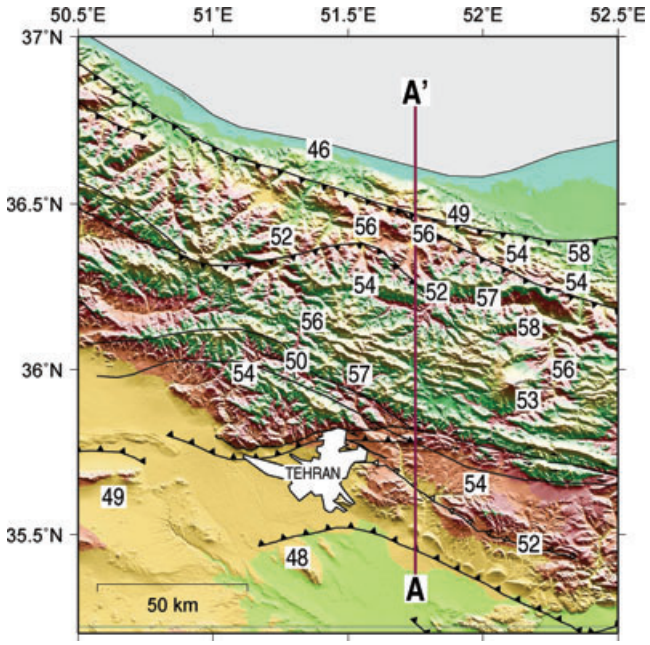

Figure 3. (a) Moho depths determined from the simultaneous inversion of receiver functions and fundamental mode Rayleigh wave group velocities. Average uncertainty in the Moho depths are estimated at ±2.5 km. The crustal cross-section shown in (b) was constructed by projecting the crustal velocity models derived from the receiver function/surface wave inversion at sites ±50 km from the line A–A′ indicated in (a) onto the profile. The upper part of the cross-section plot (b) shows the variation in topography across the Alborz Mountains from the Central Iranian Plateau to the south coast of the Caspian Sea; the middle section shows the variation in thickness of the upper and lower crust across the Alborz with the upper crust shaded and the Moho denoted by the heavy red line; and the lower part of the plot shows the individual crustal velocity models used to construct the crustal cross-section. Arrows on the individual crustal velocity models in the lower part of the figure show our interpretation of the upper/lower crust boundary and the crust–mantle boundary. The approximate relationship of the north dipping North Tehran thrust fault, the left-lateral strike-slip Mosha Fault and the south dipping Khazar thrust fault to the crustal structure are indicated on the crustal cross-section. Hypocentres of the Baladeh earthquake (Tatar *et al.* 2007) have also been projected onto the crustal cross-section.

they find little variation in crustal thickness. With a few exceptions, they find the Moho depth beneath the southern flank of the range and the Central Iranian Plateau immediately to the south to varies between 51 and 54.5 km and conclude that the Alborz Mountains have no crustal root.

Included in Table 1 are the results of Sodoudi *et al.* (2009) for three of their stations located very near to our sites. Two of the sites (K1/HSB – 4.9 km and N10/MHD – 10.8 km separation) are on the plateau south of the Alborz and the third (L1/DMV – 7.6 km separation) is near the dormant volcano Damavand. Sodoudi *et al.*'s. estimates of the Moho depth beneath HSB and MHD are 4–5 km deeper than the Moho depths we find beneath K1 and N10. The reason for the difference is that Sodoudi *et al.* (2009) use the IASPIE91 earth model (Kennett & Enghdal 1991) to convert the Moho *Ps* delay times to an interface conversion depth. The IASPIE91 model is faster (average V_s 3.81 km s^{-1}) than the average velocity we find for the central Alborz region (average V_s 3.59 km s^{-1}) resulting in a 3–4 km deeper depth estimate. In addition, we find the average V_s beneath the northern part of the Central Iranian Plateau south of the Alborz range is somewhat less (3.54 km s^{-1}) than in the central part of the range (3.60 km s^{-1}). However, Sodoudi *et al.* (2009) find the Moho beneath DMV is 13.5 km deeper than what we find for the Moho depth below L1; more than can be accounted for by the difference in V_s between the IASPIE91 and our model. Abbassi *et al.* (2010) determine the crustal thickness beneath Damavand using seismograms from the permanent broad-band seismograph located at Damavand and operated by the International Institute for Earthquake Engineering and Seismology. They find a *Ps* delay of 7 s (compared with 6.7 s at L1) and a crustal thickness of 58 ± 2 km from inverting the receiver function and the surface wave group velocity for this region (Rham 2009) (compared with 54 km beneath L1). The variation in Moho depth in the vicinity of Damavand may be due to rapid variations in crustal thickness in the immediate area of the volcano as suggested by Sodoudi *et al.* (2009), or it may be that the IASPIE91 crustal model Sodoudi *et al.* (2009) used to convert the *Ps* delay time to depth is inappropriate for this area.

Crustal thickness beneath the central Alborz Mountains is significantly greater than the 35–40 km estimated from gravity by Dehghani & Makris (1984). However, the observed ∼7 km thick root we find is thin compared to the 13–17-km-thick root required, based on typical average crust (2.82 Kg M^{-3}) and uppermost mantle (3.3 Kg M^{-3}) densities, to fully compensate the topography. Studies of earthquake focal mechanisms in the region (Priestley *et al.* 1994; Jackson *et al.* 2002; Tatar *et al.* 2007) show that the oceanic crust of the South Caspian Basin is underthrusting the Alborz Mountains from the north. Tatar *et al.* (2007) examined the main shock and aftershock locations of the 2004 Baladeh earthquake (Fig. 3) and found this earthquake involved slip on a southward dipping thrust fault, possibly the Khazar Fault, extending to ∼30 km depth. It may be that some of the topography is supported by the strong oceanic lithosphere of the South Caspian Basin. Focal mechanisms of earthquakes to the south of the range (McKenzie 1972; Jackson & McKenzie 1984; Priestley *et al.* 1994) show that the Central Iranian Plateau is underthrusting the Alborz Mountains from the south. This raises the possibility that the topography is flexurally supported.

The effective elastic thickness, T_e, is a measure of the strength of the plate and its ability to supports crustal loads over geologic time scales. T_e can be estimated from the relationship between gravity and topography in the frequency domain by computing the transfer function or admittance (McKenzie & Fairhead 1997). The gravity field of northern Iran is well constrained by observations, but the South Caspian Basin is largely devoid of measurements (Fig. 4a). Maggi *et al.* (2000) found that T_e of the Central Iranian Plateau is ∼8 km. T_e for the southern part of the South Caspian plate cannot be determined because of the lack of gravity data. However, Allen *et al.* (2002) calculated the T_e for the northern part of the South Caspian Plate immediately south of the Apsheron Sill and found a value of ∼8 km, similar to that of the Central Iranian Plateau. Except for the eastern margin of the South Caspian Basin, there is little variation in the crustal structure across the south Caspian Plate (Mangino & Priestley 1998), and therefore, it is not unreasonable to take the value of 8 km as an estimate of the T_e for the southern part of the South Caspian Plate to the north of the Alborz Mountains. There is a ∼220 mGal free-air gravity anomaly across the central Alborz (Fig. 4b). Fig. 4(c) shows the admittance for T_e of 8 km. The wavelength of the Alborz topography is 120–150 km and the average amplitude is ∼2.5 km. This gives a free-air gravity anomaly of 205–235 mGal, similar to the free-air gravity anomaly observed for the Alborz (Fig. 4b). The uncompensated admittance for the Iranian or south Caspian Plate (T_e = 8 km) is 112 mGal km^{-1}. The admittance for the Alborz is 82–95 mGal km^{-1} indicates that much of the Alborz topography is flexurally supported by the

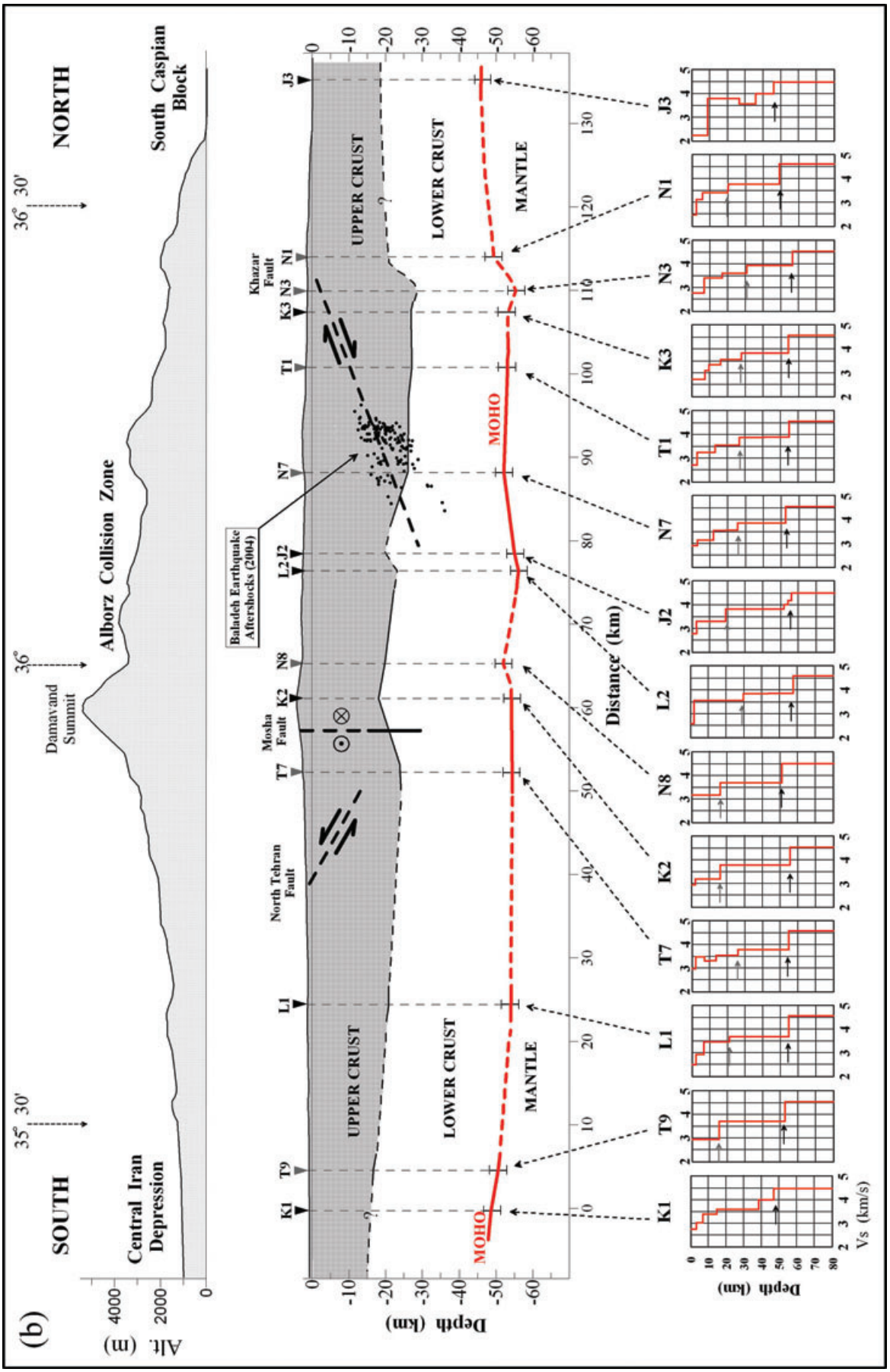

Figure 3. (*Continued.*)

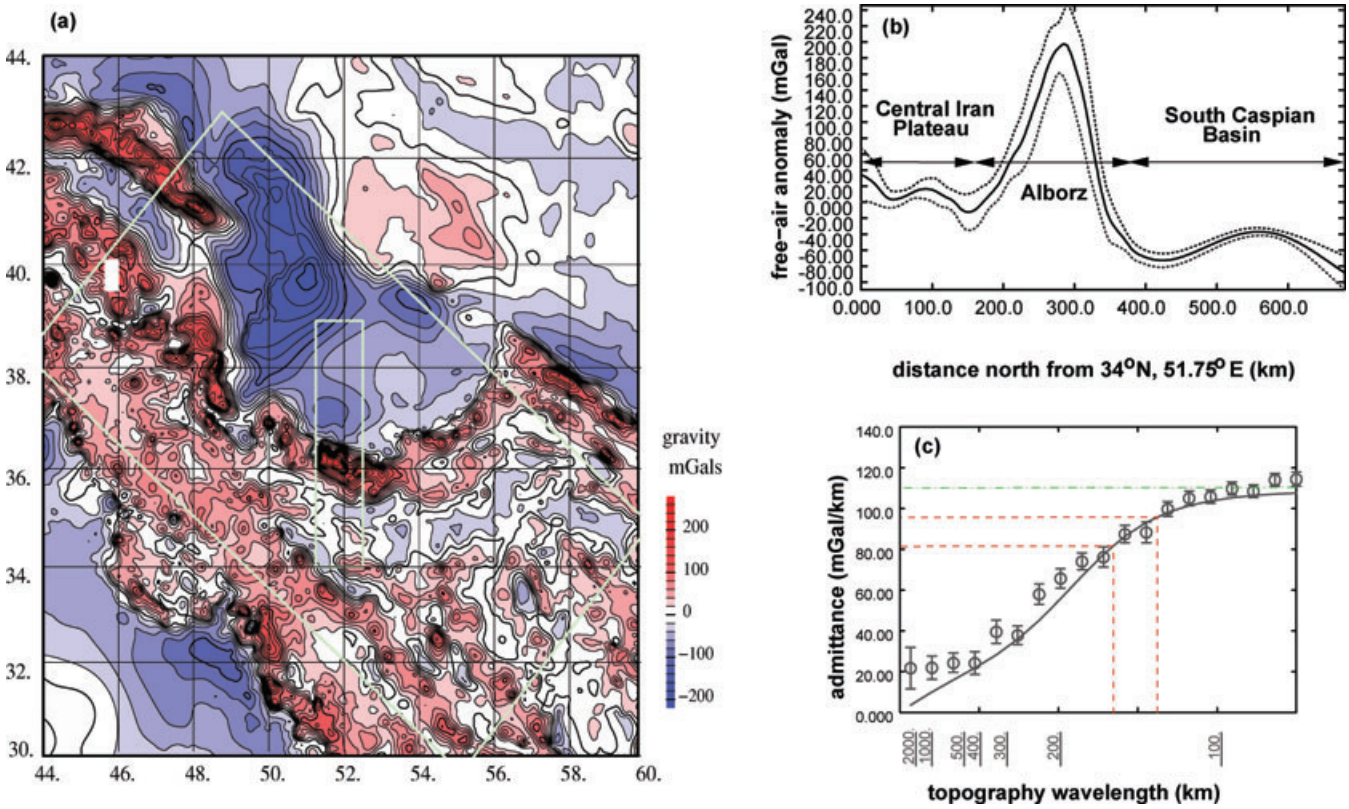

Figure 4. (a) Contoured free-air gravity for northern Iran and the South Caspian Basin. The Alborz Mountains are well-sampled by gravity measurements but there is little gravity data for the South Caspian Basin, and much of what is shown by the gravity contours in the South Caspian Basin is from interpolation. (b) Gravity profile across the central Alborz Mountains in the region of the seismic experiment. The location of the gravity profile is designated by the small, north-south light green box in (a). (c) Admittance for T_e of 8 km (Maggi *et al.* 2000) calculated for the area outlined by the oblique, light green large box in (a). The wavelength of the Alborz topography is 120–150 km (vertical red dashed lines in c) and the amplitude is ∼2.5 km giving an admittance of 82–95 mGal km^{-1}. This gives a free-air gravity anomaly of 205–235 mGal (horizontal red dashed lines in c), similar to that observed in (b). The uncompensated admittance for the Iranian or southern Caspian Plate is 112 mGal km^{-1} (horizontal green dashed-dot line in c) indicating that much of the Alborz topography is flexurally supported.

Iranian Plate, the South Caspian Plate, or both. The Alborz Mountains are too narrow and the north Iran and south Caspian plates too strong for the Alborz to form a crustal root which fully compensate the topography.

5 SUMMARY

(1) Receiver functions and surface wave group velocity data from seismograms recorded on a network of 22 broad-band seismographs have been used to determine the variation in crustal thickness across the central Alborz Mountains in northern Iran.

(2) Our analysis shows a thickening of the crust from ∼48 km beneath the northern part of the Central Iranian Plateau to 55–58 km below the central part of the Alborz Mountains, then a thinning of the crust to ∼46 km north of the Alborz Mountains beneath the coastal region of the South Caspian Sea.

(3) The crust beneath northern Iran and the central Alborz is considerably thicker that previously thought and the range does have a crustal root but significantly less than that required to full compensate the topography.

(4) Analysis of the free-air gravity anomaly across northern Iran suggest that that much of the Alborz topography is flexurally supported.

ACKNOWLEDGMENTS

Seismic instrumentation for the fieldwork described here was provided by SEISUK. This research has benefited from discussions with James Jackson and Dan McKenzie. Dan McKenzie provided the gravity and admittance plots shown in Fig. 4. James Jackson provide suggestions which considerably improved the manuscript. We thank the former president of IIEES, Prof. Ghafory-Ashtiany for his constant support. We thank Bob Herrmann who provided the receiver function/surface wave inversion routine. Figs 1 and 3(a) were made with GMT (Wessel & Smith 1998). This is Cambridge University Department of Earth Sciences contribution ES 1324.

REFERENCES

Abbassi, A., Nasrabadi, A., Tatar, M., Yaminifard, F., Abbassi, M., Hatzfeld, D. & Priestley, K., 2010. Crustal velocity structure in the southern edge of the Central Alborz (Iran), *J. Geodyn.,* **49,** 68–78.

Allen, M., Jones, S., Ismail-Zadeh, A., Simmons, M. & Anderson, L., 2002. Onset of subduction as the cause of the rapid Pliocene-Quaternary subsidence in the South Caspian basin, *Geology,* **30,** 775–778.

Allen, M., Jackson, J. & Walker, R., 2004. Late Cenozoic reorganization of the Arabia-Eurasian collision and the comparison of shhort-term and long-term deformation rates, *Tectonics,* **23,** doi:10.1029/200TC001530.

Ambraseys, N. & Melville, C.P., 1982. *A History of Persian Earthquakes,* Cambridge University Press, New York, NY, p. 219.

Asudeh, I., 1982. Seismic structure of Iran from surface and body wave data, *Geophys. J. R. astr. Soc.,* **71,** 715–730.

Axen, G., Lam, P., Grove, M., Stockli, D. & Hassanzadeh, J., 2001. Exhumation of the west-central Alborz Mountains, Iran, Caspian subsidence, and collision-related tectonics, *Geology,* **29**(6), 559–562.

Ballato, P., Nowaczyk, N., Landgraf, A., Strecker, M., Friedrich, A. & Tabatabaei, S., 2008. Tectonic control on sedimentary facies pattern and sediment accumulation rates in the Miocene foreland basin of the southern Alborz mountains, northern Iran, *Tectonics,* **27,** doi:10.1029/2008TC002278.

Berberian, M. & Yeats, R., 1999. Patterns of historical earthquake rupture in the Iranian Plateau, *Bull. seism. Soc. Am.,* **89,** 120–139.

Berberian, M., Qorashi, M., Jackson, J., Priestley, K. & Wallace, T., 1992. The Rudbar-Tarom earthquake of 20 June 1990 in NW Persia: Preliminary field and seismological observations, and its tectonic significance, *Bull. seism. Soc. Am.,* **82,** 1726–1755.

Dehghani, G. & Makris, J., 1984. The gravity field and crustal structure of Iran, *N. Jb. Geol. Paläont. Abh.,* **168,** 215–229.

Engdahl, E., Jackson, J., Myers, S., Bergman, E. & Priestley, K., 2006. Relocation and assessment of seismicity in the Iran region, *Geophys. J. Int.,* **111,** 761–778, doi:10.1029/2005JB004082.

Guest, B., Stockli, D., Grove, G., Axen, G., Lam, P. & Hassanzadeh, J., 2006. Thermal histories from the central Alborz Mountains, northern Iran: implications for the spatial and temporal distribution of deformation in northern Iran, *B. Geol. Soc. Am.,* **118,** 1507–1521.

Jackson, J. & McKenzie, D., 1984. Active tectonics of the Alpine-Himalayan belt between western Turkey and Pakistan, *Geophys. J. R. astr. Soc.,* **77,** 185–264.

Jackson, J., Priestley, K., Allen, M. & Berberian, M., 2002. Active tectonics of the South Caspian Basin, *Geophys. J. Int.,* **148**(2), 214–245.

Javan, D. & Roberts, R., 2003. Crust and uppermost mantle structure of Tehran region from analysis of teleseismic P-waveform receiver functions, *Tectonophysics,* **364,** 115–133.

Kennett, B. & Enghdal, E., 1991. Traveltimes for global earthquake location and phase identification, *Geophys. J. Int.,* **105,** 429–465.

Kennett, B., Engdahl, E. & Bulland, R., 1995. Constraints on seismic velocities in the Earth from travel times, *Geophys. J. Int.,* **122,** 108–124.

Langston, C., 1979. Structure under Mt.Rainier, Washington, inferred from teleseismic body waves, *J. geophys. Res.,* **84,** 4749–4762.

Ligorria, J. & Ammon, C., 1999. Iterative deconvolution and receiver-function estimation, *Bull. seism. Soc. Am.,* **89,** 1395–1400.

Maggi, A., Jackson, J., McKenzie, D. & Priestley, K., 2000. Earthquake focal depths, effective elastic thickness, and the strength of the continental lithosphere, *Geology,* **28,** 495–498.

Mangino, S. & Priestley, K., 1998. The crustal structure of the southern Caspian region, *Geophys. J. Int.,* **133,** 630–648.

McKenzie, D., 1972. Active tectonics of the Mediterranean region, *Geophys. J. R. astr. Soc.,* **30,** 109–185.

McKenzie, D. & Fairhead, D., 1997. Estimates of the effective elastic thickness of the continental lithosphere from Bouger and free air gravity anomalies, *J. geophys. Res.,* **102,** 27 523–27 552.

Paul, A., Kaviani, A., Hatzfeld, D., Vergne, J. & Mokhtari, M., 2006. Seismological evidence for crustal-scale thrusting in the Zagros mountain belt(Iran), *Geophys. J. Int.,* **166,** 227–237.

Priestley, K., Baker, C. & Jackson, J., 1994. Implications of earthquake focal mechanism data for the active tectonics of the south Caspian Basin and surrounding regions, *Geophys. J. Int.,* **118,** 111–141.

Rham, D., 2009. The crustal structure of the Middle East, *PhD thesis*, University of Cambridge Library, Cambridge, UK.

Ritz, J.-F., Nazari, N., Ghassemi, A., Salamati, R., Shafei, A., Solaymani, S. & Vernant, P., 2006. Active transtention inside central Alborz: a new insight into northern Iran-south Caspian geodynamics, **34,** 477–480.

Sodoudi, F., Yuan, X., Kind, R., Heit, B. & Sadidkhouy, A., 2009. Evidence for a missing crustal root and a thin lithosphere beneath the Central Alborz by receiver function studies, *Geophys. J. Int.,* **177,** 733–742, doi:10.1111/j.1365-246X.2009.04115.x.

Tatar, M., Jackson, J., Hatzfeld, D. & Bergman, E., 2007. The 2004 May 28 Baladeh earthquake (mw 6.2) in the Alborz, Iran: overthrusting the South Caspian Basin margin, partitioning of oblique convergence and the seismic hazard of Tehran, *Geophys. J. Int.,* **170,** 249–261.

Vernant, P. *et al.*, 2004. Present-day crustal deformation and plate kinematics in Middle East constrained by GPS measurements in Iran and northern Oman, *Geophys. J. Int.,* **157,** 381–398.

Wessel, P. & Smith, W., 1998. New, versions of the generic mapping tool released, *EOS, Trans. Am. geophys. Un.,* **79,** 579.

APPENDIX

Figs A1–A4 can be seen on the following pages.

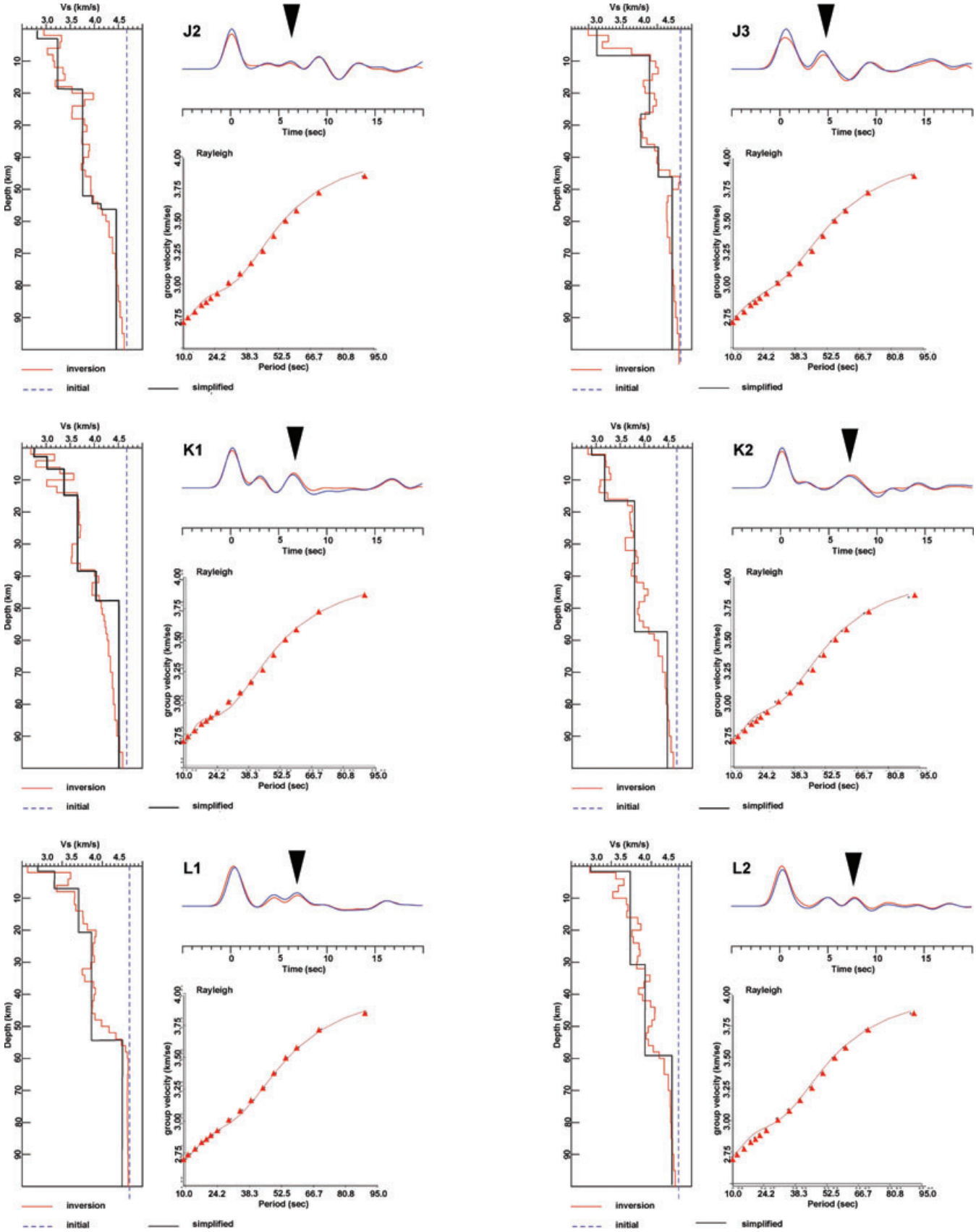

Figure A1. Receiver function and surface wave analysis for the sites J2, J3, K1, K2, L1 and L2. The number of receiver function stacks inverted and the total number of receiver function included in the receiver function stacks is given in Table 1. The format of the figure is the same as that in Fig. 2.

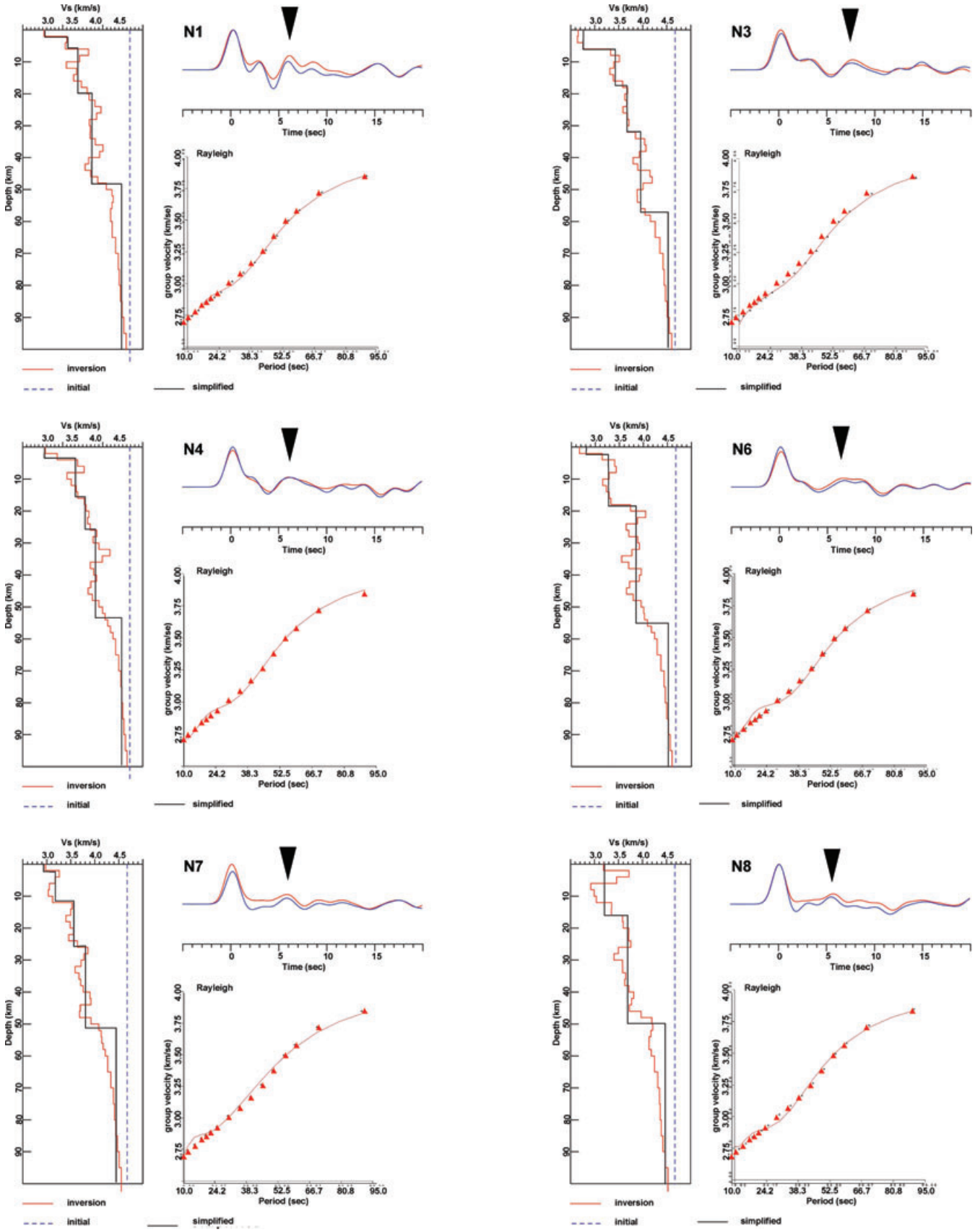

Figure A2. Receiver function and surface wave analysis for the sites N1, N3, N4, N6, N7 and N8. The number of receiver function stacks inverted and the total number of receiver function included in the receiver function stacks is given in Table 1. The format of the figure is the same as that in Fig. 2.

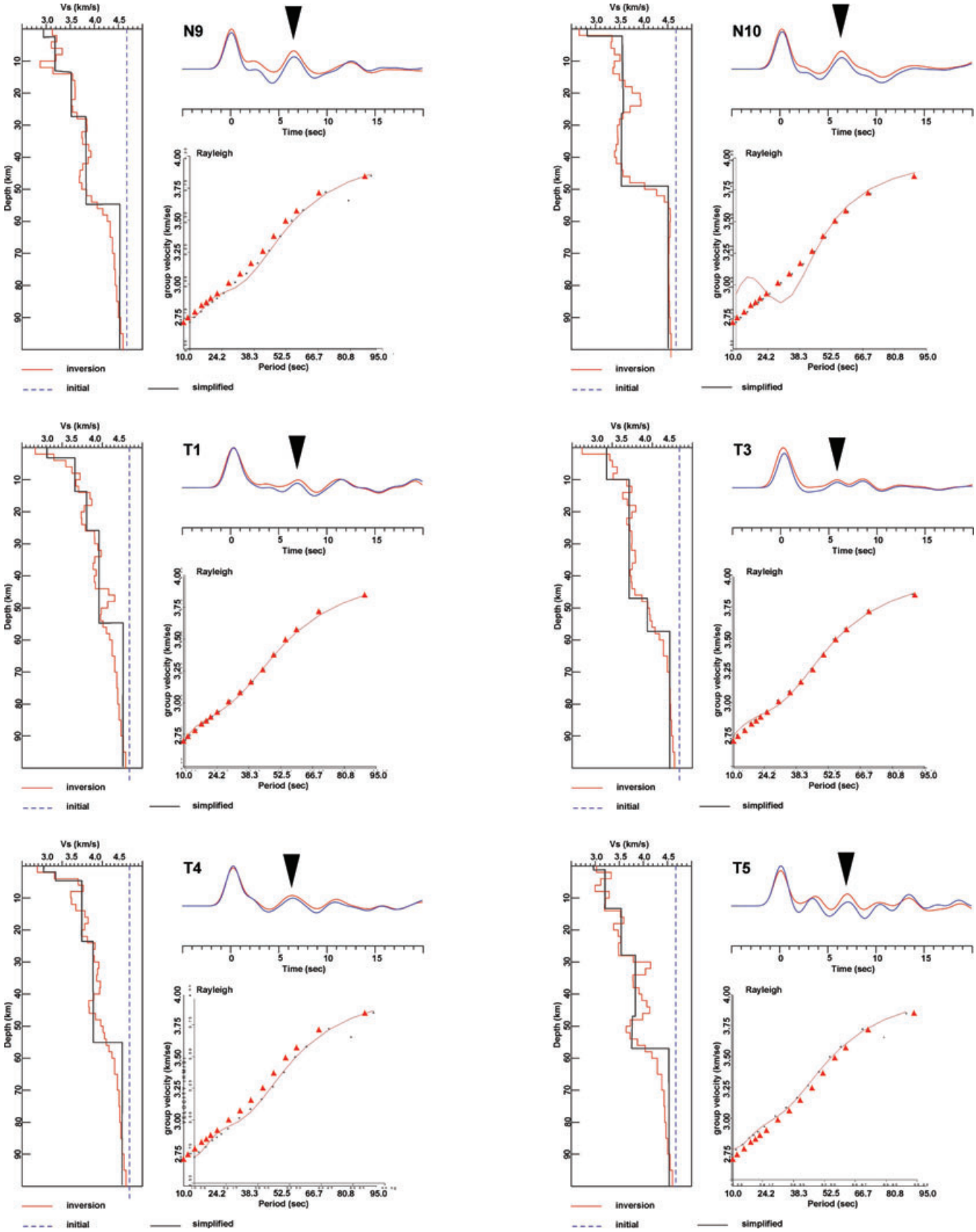

Figure A3. Receiver function and surface wave analysis for the sites N9, N10, T1, T3, T4 and T5. The number of receiver function stacks inverted and the total number of receiver function included in the receiver function stacks is given in Table 1. The format of the figure is the same as that in Fig. 2.

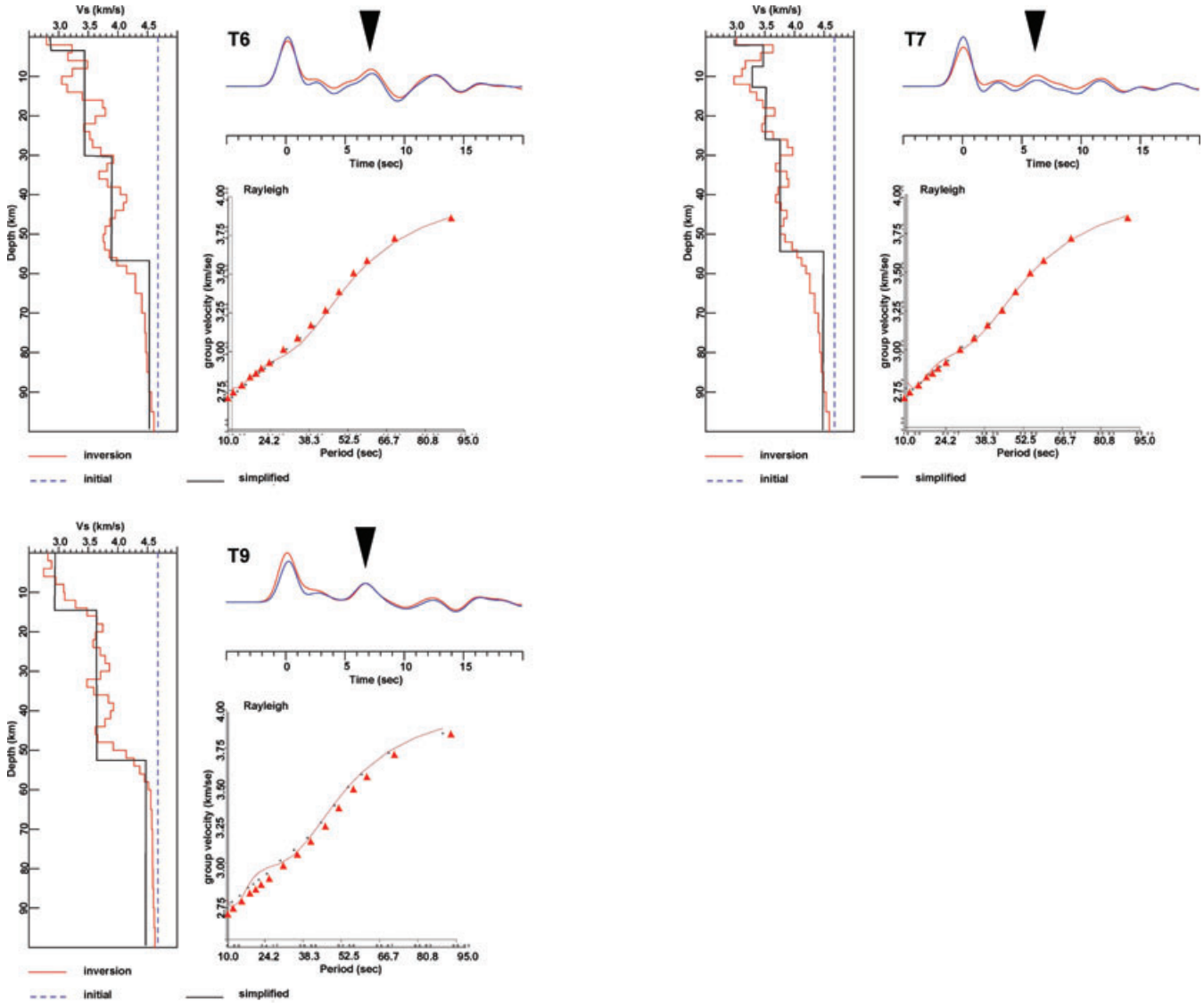

Figure A4. Receiver function and surface wave analysis for the sites T6, T7 and T9. The number of receiver function stacks inverted and the total number of receiver function included in the receiver function stacks is given in Table 1. The format of the figure is the same as that in Fig. 2.